Gated based quantum computer algorithm for geophysical inversion

Jorge E. Monsegny and Daniel Trad, CREWES University of Calgary; Don C. Lawton, University of Calgary and Carbon Management Canada*

SUMMARY

We want to show a framework to solve geophysical inversion problems using a gated based quantum computer. The resultant quantum algorithm belongs to the quantum search algorithm class where the query is a forward modelling calculation, and we look for the minimum residual. This quantum algorithm can find the global minimum in $O(\sqrt{N})$ queries where N is the number of models. This algorithm does not need gradient or Hessian calculations, only forward modelling, and residuals calculation. We illustrate the algorithm with a small instance of a traveltime tomography problem.

INTRODUCTION

In 1981 quantum computation was proposed by Richard Feynman to simulate quantum systems (Preskill, 2021). Later, in 1985, David Deutsch extended the notion of quantum computer to problems not related to quantum physics (Deutsch and Penrose, 1985).

Several applications appeared in the following decade showing that quantum computing is more powerful than classical computing. For example, an exponential speedup was found in the period finding problem (Simon, 1994) that inspired the Shor algorithm for factoring large numbers (Shor, 1997) that threatens cryptological systems. The quantum searching algorithm that inspires the algorithm proposed in this report is also from that decade (Grover, 1997) and its speedup is quadratic.

Some applications of quantum computing to geophysical problems have been proposed in the last 10 years. Most of them use a less powerful technique called quantum annealing (de Falco and Tamascelli, 2011). Only in the last couple of years general quantum computing algorithms have been proposed in geophysical problems. Alulaiw and Sen (2015) find that quantum annealing is faster than the simulated annealing and does not get trapped in local minima when performing seismic prestack inversion. Moradi et al. (2018) present the different quantum computing concepts necessary for wave modelling applications in geophysics.

Sarkar and Levin (2018) use quantum annealing to estimate the rock material percentages with traveltime information. Greer and O'Malley (2020) introduce a quantum annealing algorithm to solve constrained optimization problems and applies it to invert the subsurface P-wave velocity. van der Linde (2021) solves the residual statics problem using quantum annealing and quantum-classic hybrid solvers. In Souza et al. (2022) the velocities of a layered model are inverted using quantum annealing techniques. Albino et al. (2022) solve the same problem with variational quantum algorithm.

This expanded abstract is structured as follows. First we describe the classical algorithm for geophysical inversion that calls the main quantum circuit. Then we show an instance of this quantum circuit tailored for traveltime tomography and a small example. At the end we discuss the results and present some conclusions. It is challenging to introduce the basic quantum computing theory in an expanded abstract, so we will mention the important aspects and give references. A very good introductory book is Johnston (2019).

METHODS

Quantum computers work with quantum bits instead of bits like classical computers. The main difference is that a bit can be in two mutually exclusive states, 0 or 1, while a qubit can be in a combination of states $|0\rangle$ and $|1\rangle$, pronounced "ket". This superposition extends exponentially the number of states a set of qubits can be in. For example, 8 bits can be in only one of 256 states while 8 qubits can be in the 256 states simultaneously. The idea is to use qubits for the model we want to invert and perform all the calculations in parallel.

A superposition of $|0\rangle$ and $|1\rangle$ means a linear combination $\alpha|0\rangle + \beta|1\rangle$ where α and β are complex numbers such that $|\alpha|^2 + |\beta|^2 = 1$. This last condition of the scalars α and β is related to the act of measuring, or reading in computer parlance, a qubit. Sets of qubits can be grouped and interpreted as number in the same way bits are grouped to for integers and floating point numbers (Johnston, 2019).

In quantum computation the work is done by quantum gates that operate on single or multiple qubits. It is possible to perform multiplications, summations, and other arithmetic operations with them. More importantly, they operate simultaneously in all the states of a set of quantum qubits. With them it is possible to perform forward modelling and residuals calculation in a superposition of velocity models in a quantum parallel way.

An example gate is the negation or X-gate that interchanges $|0\rangle$ with $|1\rangle$:

$$\alpha|0\rangle + \beta|1\rangle \;—\boxed{X}—\; \alpha|1\rangle + \beta|0\rangle$$

More gates and the implementation of arithmetic circuits with them can be found in Johnston (2019) and Vedral et al. (1996).

The next step is to look for the minimum of the residual's superposition using a quantum search algorithm. A limitation of quantum computing is that after the calculations in superposition are performed, only one of the answers can be measured, randomly. To overcome this limitation, it is possible to increase the probability of the answer we are looking for. The Grover's quantum searching algorithm is a way to increase the probability of the model with the minimum residual, so it can be measured at the end. This circuit, also called mirror, can be found in Johnston (2019).

The main algorithm runs in a classical computer but calls the main quantum circuit.This algorithm is based in the quantum minimum search algorithm of Durr and Hoyer (1999) that uses the general searching algorithms of Boyer et al. (1998). The pseudocode is shown Algorithm 1.

Algorithm 1: Main optimization algorithm. It runs classically in a conventional computer but calls the quantum function `quantum_circuit` that performs the quantum optimization stage.

Data: Initial model v_0, parameters d and measured data t.
Result: Global minimum v.

$v \leftarrow v_0$
$r \leftarrow \texttt{classical\_misfit}(v)$
$outter\_steps \leftarrow 0$
while $outter\_steps < \texttt{max\_steps}(N)$ **do**
  $n \leftarrow 1, \lambda \leftarrow 8/7, inner\_steps \leftarrow 0$
  while $inner\_steps < \texttt{max\_iter}(N)$ **do**
    $j \leftarrow \lfloor \texttt{uniform}(0,n) \rfloor$
    $inner\_steps \leftarrow inner\_steps + j$
    $outter\_steps \leftarrow outter\_steps + j$
    `// This is the only quantum call`
    $v' \leftarrow \texttt{quantum\_circuit}(j,d,t,r)$
    $r' \leftarrow \texttt{classical\_misfit}(v')$
    if $r' < r$ **then break**
    else $n \leftarrow \texttt{min}(\lambda n, \sqrt{N})$
  if $r' < r$ **then** $r \leftarrow r', v \leftarrow v'$
return v

The inputs are an initial model v_0, modelling parameters d and the measured data t. The first part consists in calculating, classically, the misfit of the initial model that will be used as the initial reference misfit r. The rest of the algorithm is composed of two nested loops. The external one runs for a number of iterations that is function of the number of possible models N. A tight upperbound of this value was found in Durr and Hoyer (1999):

$$\texttt{max\_steps}(N) = 22.5\sqrt{N} + 1.4\log^2 N \tag{1}$$

The internal loop runs for a different number of iterations that is also a function of N. This number was estimated in Boyer et al. (1998):

$$\texttt{max\_iter}(N) = \frac{9}{4}\sqrt{N} \tag{2}$$

The main quantum circuit is called from inside the inner loop with a number j of basic steps. This number is chosen randomly between 0 and n, with the value of n starting equal to one at each external iteration but increasing at a rate dictated by $\lambda = 8/7$ during each internal iteration. The number of outer and inner steps is incremented by j.

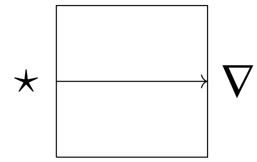

Figure 1: Tomography example configuration. It is composed of a single slowness cell, a source ($\star$) and a receiver (∇).

Apart from j, the main quantum circuit is called with the modelling parameters d, the measured data t and the reference misfit r. At each invocation of this quantum circuit the superposition of models is initialized again. Its output is a model v' that might or might not have a misfit smaller than r. The algorithm only knows v' so it calculates, classically, its misfit r'. If this misfit is less than r we exit the internal loop. If not, we increase the maximum number of basic steps n.

When the inner loop finishes, the algorithm updates the reference misfit r and current model v if the new misfit is less than the previous one.

Durr and Hoyer (1999) found that this strategy of increasing gradually the number of basic steps and calling multiple times the main quantum circuit needs less total basic steps than just calling once at the beginning the main quantum circuit. It also avoids the possibility of iterating too many times and missing the maximum probability the Mirror circuit can achieve.

EXAMPLE

Now we present a step by step simulation of the main quantum circuit configured for traveltime tomography. We use the most simple tomography problem to keep calculations and diagrams small. It is the problem with a single cell and a single time measurement between source and receiver, as in Figure 1. The ray length is 2 units and the traveltime measurement is 4 units.

Figure 3 shows part of the circuit for this problem. The part of the circuit not shown undoes the computation of the part shown, except the phase inversion. Line d and v have 2 qubits each one and will be interpreted as unsigned integers. With this number of qubits they can express 4 numbers from 0 to 3. The other lines, t^*, tr and r^*, have 4 qubits each one and will be interpreted as signed integers. They can express numbers from -8 to 7.

The Table 1 shows the computation states of the circuit in Figure 3. The numbers under the column stage correspond to the numbers at the top of the circuit. The other columns have the contents of each qubit line in the circuit. We swapped tr and r^* for convenience.

By convention all qubits are $|0\rangle$ at stage 0. During stage 1 the superposition of all possible models is created in v using Hadamard gates. For convenience we distribute, using the tensor product rules, r^* and t^* over v in the next row, also labelled stage 1. In stage 2 the ray length is input in d. During stage 3 the multiplication of d and v is performed in parallel and stored

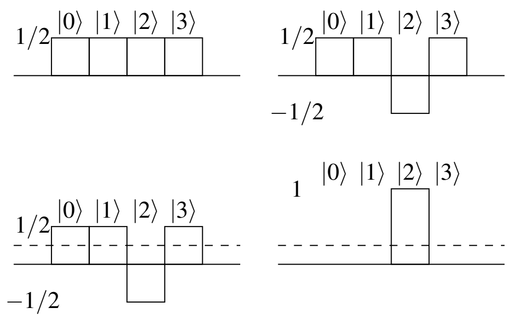

Figure 2: Mirror stage effect on the velocity models superposition in register v. At the beginning all the probabilities are equal but the quantum circuit flips the phase of the minimum (top row). The mirror circuit rotates the probabilities around the mean increasing the probability of the minimum (bottom row).

in t^*. The next stage introduces the negative of the measured data, -4, in tr.

Stage 5 adds tr to t^* and the following stage takes the absolute value of t^*. At this point the residuals of every possible model are in t^*. The stage 7 adds the residuals to the total calculated misfit in r^*. Stages 8 to 12 undo stages 2-6, preserving the total misfit in r^*. In stage 13 the negative of reference misfit, -1 in this example, is entered in tr. Notice that only one term in the superposition has r^* smaller than the reference misfit. The next stage adds tr to r^*. Now the term with misfit less than the reference one is the only with a negative value.

During stage 15 the circuit flips the phase of all the terms with negative r^*. This phase is the key because it marks the term with the minimum. The following stages are not in the table nor in the circuit but they undo all computation performed in stages 2 to 14. The result is in the last row of the table. It is almost the same as row 1, except that the term with the minimum has a negative phase while the other terms have a positive one.

The next step is to apply the Mirror circuit. Figure 2 shows the effect of the Mirror circuit on the final superposition v. The signed coefficients are 0.5 for terms $|0\rangle$, $|1\rangle$ and $|3\rangle$, while it is -0.5 for $|2\rangle$. The coefficients mean is 0.25. After using the mean as a rotation axis, $|2\rangle$ ends with a coefficient equal to 1 and the other terms with 0. If we read the contents of v right now, we will obtain $|2\rangle$, the answer to this optimization problem.

There is no need to iterate more times due to the size of this problem instance. Instances of this problem with bigger models will need more iterations to obtain the answer at the end.

DISCUSSION

The main attractive of using quantum computation for solving inverse problems is using quantum superposition. With quantum superposition we can calculate the residuals of a set of geophysical models in parallel. The main drawback is that it is not possible to read all of them but just one, depending on the coefficients of the quantum superposition. It is necessary to increase the probability of one term, the one corresponding to the inversion solution, by applying the mirror or Grover's iteration several times. This approach is the same used in quantum searching algorithms (Grover, 1997) and requires around $O(\sqrt{N})$ iterations when N models are simulated in superposition. It is still a huge advantage because it allows to explore the model space with the same number of iterations of a single gradient based inversion.

In addition, the actual computation done in superposition is simpler than the classical one because there is no need to compute gradients or Hessians. Only forward modelling and residual calculation are needed, and this simplifies the quantum operations.

Classical computers use floating point formats to encode the inverted models and perform the optimization. In the quantum computing case, the number of available qubits, that is scarce for the moment, constraints the range and precision of the numbers in the quantum calculations. We used very few qubits and a very small problem to test the concept of quantum inversion and because simulating a quantum computer with a classical one is computationally expensive. However, there are reports that predict up to thousands or even millions of qubits by the end of this decade (IBM Computing, 2021; Google, 2022). Although this refers to physical qubits and not logical qubits, the increase in the size of the applications will be worthwhile.

The traveltime tomography with fixed raypaths required a simple forward modelling. More complex modellings, like full wave simulations, are still a challenge due to their complexity. In quantum computing every operation should be reversible, because quantum systems are, and this means that more effort has to be spent in coding numerical computations in quantum terms. Future quantum compilers can leverage this issue, though.

ACKNOWLEDGEMENTS

We thank the sponsors of CREWES for continued support. This work was funded by CREWES industrial sponsors and NSERC (Natural Science and Engineering Research Council of Canada) through the grant CRDPJ 543578-19. The data were acquired through a collaboration with Containment and Monitoring Institute (CaMI) of Carbon Management Canada (CMC). Research at the CaMI field site is supported in part by the Canada First Research Excellence Fund, through the Global Research Initiative at the University of Calgary and the CaMI.FRS Joint Industry Project. The first author (JM) is also supported by Canada First Research Excellence Fund, through the Global Research Initiative at the University of Calgary

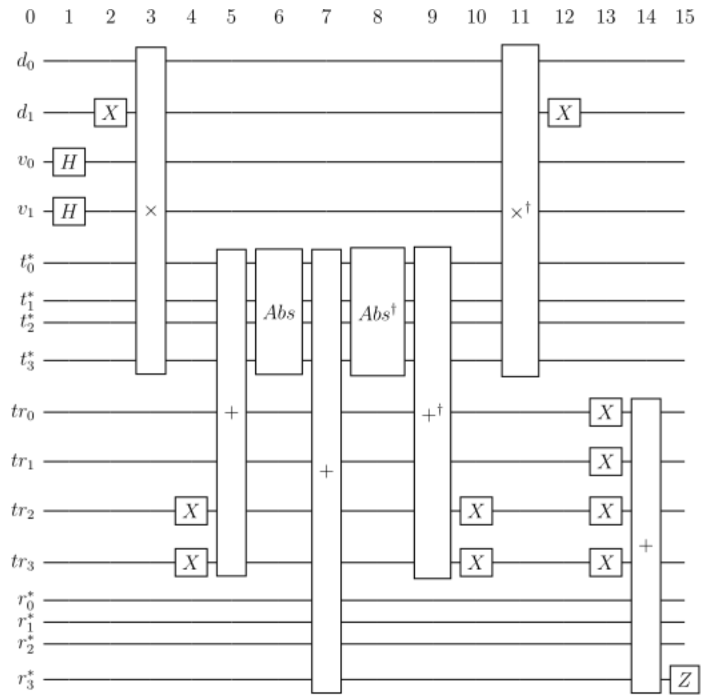

Figure 3: Quantum circuit for tomography. Quantum registers are d for ray lengths, v for velocities, t^* for calculated traveltimes, tr for measured traveltimes and test misfits, and r^* for calculated misfits. The numbers above are for cross reference with Table 1.

<table>
<tr><th>Stage</th><th>tr</th><th>r^*</th><th>t^*</th><th>v</th><th>d</th></tr>
<tr><td>0</td><td>$\|0\rangle$</td><td>$\|0\rangle$</td><td>$\|0\rangle$</td><td>$\|0\rangle$</td><td>$\|0\rangle$</td></tr>
<tr><td>1</td><td>$\|0\rangle$</td><td>$\|0\rangle$</td><td>$\|0\rangle$</td><td>$\frac{1}{2}\|0\rangle+\frac{1}{2}\|1\rangle+\frac{1}{2}\|2\rangle+\frac{1}{2}\|3\rangle$</td><td>$\|0\rangle$</td></tr>
<tr><td>1</td><td>$\|0\rangle$</td><td colspan="3">$\frac{1}{2}\|000\rangle+\frac{1}{2}\|001\rangle+\frac{1}{2}\|002\rangle+\frac{1}{2}\|003\rangle$</td><td>$\|0\rangle$</td></tr>
<tr><td>2</td><td>$\|0\rangle$</td><td colspan="3">$\frac{1}{2}\|000\rangle+\frac{1}{2}\|001\rangle+\frac{1}{2}\|002\rangle+\frac{1}{2}\|003\rangle$</td><td>$\|2\rangle$</td></tr>
<tr><td>3</td><td>$\|0\rangle$</td><td colspan="3">$\frac{1}{2}\|000\rangle+\frac{1}{2}\|021\rangle+\frac{1}{2}\|042\rangle+\frac{1}{2}\|063\rangle$</td><td>$\|2\rangle$</td></tr>
<tr><td>4</td><td>$\|-4\rangle$</td><td colspan="3">$\frac{1}{2}\|000\rangle+\frac{1}{2}\|021\rangle+\frac{1}{2}\|042\rangle+\frac{1}{2}\|063\rangle$</td><td>$\|2\rangle$</td></tr>
<tr><td>5</td><td>$\|-4\rangle$</td><td colspan="3">$\frac{1}{2}\|0(-4)0\rangle+\frac{1}{2}\|0(-2)1\rangle+\frac{1}{2}\|002\rangle+\frac{1}{2}\|023\rangle$</td><td>$\|2\rangle$</td></tr>
<tr><td>6</td><td>$\|-4\rangle$</td><td colspan="3">$\frac{1}{2}\|040\rangle+\frac{1}{2}\|021\rangle+\frac{1}{2}\|002\rangle+\frac{1}{2}\|023\rangle$</td><td>$\|2\rangle$</td></tr>
<tr><td>7</td><td>$\|-4\rangle$</td><td colspan="3">$\frac{1}{2}\|440\rangle+\frac{1}{2}\|221\rangle+\frac{1}{2}\|002\rangle+\frac{1}{2}\|223\rangle$</td><td>$\|2\rangle$</td></tr>
<tr><td>8</td><td>$\|-4\rangle$</td><td colspan="3">$\frac{1}{2}\|4(-4)0\rangle+\frac{1}{2}\|2(-2)1\rangle+\frac{1}{2}\|002\rangle+\frac{1}{2}\|223\rangle$</td><td>$\|2\rangle$</td></tr>
<tr><td>9</td><td>$\|-4\rangle$</td><td colspan="3">$\frac{1}{2}\|400\rangle+\frac{1}{2}\|221\rangle+\frac{1}{2}\|042\rangle+\frac{1}{2}\|263\rangle$</td><td>$\|2\rangle$</td></tr>
<tr><td>10</td><td>$\|0\rangle$</td><td colspan="3">$\frac{1}{2}\|400\rangle+\frac{1}{2}\|221\rangle+\frac{1}{2}\|042\rangle+\frac{1}{2}\|263\rangle$</td><td>$\|2\rangle$</td></tr>
<tr><td>11</td><td>$\|0\rangle$</td><td colspan="3">$\frac{1}{2}\|400\rangle+\frac{1}{2}\|201\rangle+\frac{1}{2}\|002\rangle+\frac{1}{2}\|203\rangle$</td><td>$\|2\rangle$</td></tr>
<tr><td>12</td><td>$\|0\rangle$</td><td colspan="3">$\frac{1}{2}\|400\rangle+\frac{1}{2}\|201\rangle+\frac{1}{2}\|002\rangle+\frac{1}{2}\|203\rangle$</td><td>$\|0\rangle$</td></tr>
<tr><td>13</td><td>$\|-1\rangle$</td><td colspan="3">$\frac{1}{2}\|400\rangle+\frac{1}{2}\|201\rangle+\frac{1}{2}\|002\rangle+\frac{1}{2}\|203\rangle$</td><td>$\|0\rangle$</td></tr>
<tr><td>14</td><td>$\|-1\rangle$</td><td colspan="3">$\frac{1}{2}\|300\rangle+\frac{1}{2}\|101\rangle+\frac{1}{2}\|(-1)02\rangle+\frac{1}{2}\|103\rangle$</td><td>$\|0\rangle$</td></tr>
<tr><td>15</td><td>$\|-1\rangle$</td><td colspan="3">$\frac{1}{2}\|300\rangle+\frac{1}{2}\|101\rangle-\frac{1}{2}\|(-1)02\rangle+\frac{1}{2}\|103\rangle$</td><td>$\|0\rangle$</td></tr>
<tr><td></td><td></td><td colspan="3">$\vdots$</td><td></td></tr>
<tr><td>End</td><td>$\|0\rangle$</td><td>$\|0\rangle$</td><td>$\|0\rangle$</td><td>$\frac{1}{2}\|0\rangle+\frac{1}{2}\|1\rangle-\frac{1}{2}\|2\rangle+\frac{1}{2}\|3\rangle$</td><td>$\|0\rangle$</td></tr>
</table>

Table 1: Computation states of the tomography circuit if Figure 3. The numbers in the column stage refer to the numbers on top of that figure. Each column is the state of one of the circuit registers. For convenience some registers are gather together. The important outcome is that the sign of the minimum, $|2\rangle$, has been flipped so the mirror circuit can increase its probability to be measured.

REFERENCES

Albino, A., O. Pires, R. Ferreira de Souza, P. Santos, A. Neto, and E. G. Sperandio Nascimento, 2022, Employing gate-based quantum computing for traveltime seismic inversion: Presented at the .

Alulaiw, B., and M. K. Sen, 2015, *in* Prestack Seismic Inversion by Quantum Annealing: 3507–3511.

Boyer, M., G. Brassard, P. Høyer, and A. Tapp, 1998, Tight bounds on quantum searching: Fortschritte der Physik, **46**, 493–505; doi: 10.1002/(sici)1521-3978(199806)46:4/5¡493::aid-prop493¿3.0.co;2-p.

de Falco, D., and D. Tamascelli, 2011, An introduction to quantum annealing: RAIRO - Theoretical Informatics and Applications, **45**; doi: 10.1051/ita/2011013.

Deutsch, D., and R. Penrose, 1985, Quantum theory, the church–turing principle and the universal quantum computer: Proceedings of the Royal Society of London. A. Mathematical and Physical Sciences, **400**, 97–117; doi: 10.1098/rspa.1985.0070.

Durr, C., and P. Hoyer, 1999, A quantum algorithm for finding the minimum.

Google, 2022, Our quantum computing journey.

Greer, S., and D. O'Malley, 2020, *in* An approach to seismic inversion with quantum annealing: 2845–2849.

Grover, L. K., 1997, Quantum mechanics helps in searching for a needle in a haystack: Physical Review Letters, **79**; doi: 10.1103/PhysRevLett.79.325.

IBM Computing, 2021, IBM's roadmap for building an open quantum software ecosystem.

Johnston, E. R., 2019, Programming quantum computers : essential algorithms and code samples, first edition. ed.: O'Reilly.

Moradi, S., D. Trad, and K. A. Innanen, 2018, *in* Quantum computing in geophysics: Algorithms, computational costs, and future applications: 4649–4653.

Preskill, J., 2021, Quantum computing 40 years later.

Sarkar, R., and S. A. Levin, 2018, Snell tomography for net-to-gross estimation using quantum annealing: Presented at the . (SEG-2018-2998409).

Shor, P. W., 1997, Polynomial-time algorithms for prime factorization and discrete logarithms on a quantum computer: SIAM J. Comput., **26**, 1484–1509; doi: 10.1137/S0097539795293172.

Simon, D., 1994, On the power of quantum computation: Proceedings 35th Annual Symposium on Foundations of Computer Science, 116–123.

Souza, A. M., E. O. Martins, I. Roditi, N. Sá, R. S. Sarthour, and I. S. Oliveira, 2022, An application of quantum annealing computing to seismic inversion: Frontiers in Physics, **9**; doi: 10.3389/fphy.2021.748285.

van der Linde, S., 2021, Quantum annealing for seismic imaging: Exploring quantum annealing possibilities for residual statics estimation using the d-wave advantage system and hybrid solver: Master's thesis, Delft University of Technology.

Vedral, V., A. Barenco, and A. Ekert, 1996, Quantum networks for elementary arithmetic operations: Physical Review A, **54**, 147–153; doi: 10.1103/physreva.54.147.